AIP Advances

High electrical conductivity in out of plane direction of electrodeposited Bi_2Te_3 films

Cite as: AIP Advances 5, 087142 (2015); https://doi.org/10.1063/1.4928863
Submitted: 18 May 2015 . Accepted: 03 August 2015 . Published Online: 14 August 2015

Miguel Muñoz Rojo, Cristina V. Manzano, Daniel Granados, M. R. Osorio, Theodorian Borca-Tasciuc, and Marisol Martín-González

COLLECTIONS

Paper published as part of the special topic on Chemical Physics, Energy, Fluids and Plasmas, Materials Science and Mathematical Physics

View Online

Export Citation

CrossMark

ARTICLES YOU MAY BE INTERESTED IN

Method for Measuring Electrical Resistivity of Anisotropic Materials
Journal of Applied Physics 42, 2971 (1971); https://doi.org/10.1063/1.1660656

Thermal conductivity measurement from 30 to 750 K: the 3ω method
Review of Scientific Instruments 61, 802 (1990); https://doi.org/10.1063/1.1141498

Finite element and analytical solutions for van der Pauw and four-point probe correction factors when multiple non-ideal measurement conditions coexist
Review of Scientific Instruments 88, 094704 (2017); https://doi.org/10.1063/1.5001830

AIP Advances
Fluids and Plasmas Collection

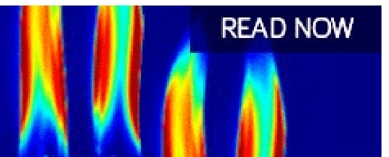

AIP Publishing

© 2015 Author(s).

AIP ADVANCES **5**, 087142 (2015)

High electrical conductivity in out of plane direction of electrodeposited Bi_2Te_3 films

Miguel Muñoz Rojo,[1] Cristina V. Manzano,[1] Daniel Granados,[2]
M. R. Osorio,[2] Theodorian Borca-Tasciuc,[3] and Marisol Martín-González[1]
[1] *IMM-Instituto de Microelectrónica de Madrid(CNM-CSIC), Isaac Newton 8,PTM, E- 28760Tres Cantos, Madrid, Spain*
[2] *IMDEA Nanoscience, Faraday, 9, Ciudad Universitaria de Cantoblanco, 28049, Madrid, Spain*
[3] *Rensselaer Polytechnic Institute (RPI), 110 8th St, Troy, NY 12180, United States*

(Received 18 May 2015; accepted 3 August 2015; published online 14 August 2015)

The out of plane electrical conductivity of highly anisotropic Bi_2Te_3 films grown via electro-deposition process was determined using four probe current-voltage measurements performed on 4.6 - 7.2 μm thickness Bi_2Te_3 mesa structures with 80 - 120 μm diameters sandwiched between metallic film electrodes. A three-dimensional finite element model was used to predict the electric field distribution in the measured structures and take into account the non-uniform distribution of the current in the electrodes in the vicinity of the probes. The finite-element modeling shows that significant errors could arise in the measured film electrical conductivity if simpler one-dimensional models are employed. A high electrical conductivity of $(3.2 \pm 0.4) \cdot 10^5$ S/m is reported along the out of plane direction for Bi_2Te_3 films highly oriented in the [1 1 0] direction. © *2015 Author(s). All article content, except where otherwise noted, is licensed under a Creative Commons Attribution 3.0 Unported License.* [http://dx.doi.org/10.1063/1.4928863]

I. INTRODUCTION.

Bismuth telluride (Bi_2Te_3)[1] is a semiconductor material that is especially well-known for its application in thermoelectric devices at room temperature. The efficiency of these materials is related to its figure of merit, which is defined in terms of the fundamental transport properties of the material, i.e. $zT = ((\sigma \cdot S^{2)}/k) \cdot T$ where S is the Seebeck coefficient and σ and k are the electrical and thermal conductivity, respectively. In the last decade, there has been a great interest in improving its thermoelectric efficiency through nano-structuration, like 2D- or 1D-structures. Measurements of the transport properties of the material are mandatory in order to quantify what the impact of such spatial confinement is on its thermoelectric efficiency. However, the measurements of the transport properties of these structures at the nano-scale are not trivial, requiring of specific equipment and/or careful analysis.[2,3]

Bi_2Te_3 is also a very anisotropic material, presenting different transport properties in its different directions. Therefore, measurements on different directions might result in very different values. Among the different transport properties that must be characterized, the electrical conductivity is a key parameter in the thermoelectric efficiency of these films and determining it in the out of plane direction, which is the typical working orientation in thermoelectric devices, is fundamental to obtain its figure of merit. In this work, Bi_2Te_3 films (2D-structures) were grown through electrodeposition and its electrical conductivity was determined in its out of plane direction.

Electrical resistivity measurements of films are of major concern in many applications, like solar cells,[4] electrical circuits[5] or thermoelectric devices[6] among others. As an example, thermoelectric materials,[6] which are able to transform heat into electricity and vice-versa, require accurate measurements of the electrical conductivity of the film in order to determine the thermoelectric figure of merit of the material.

 ©Author(s) 2015

There are a wide variety of techniques that can be used to measure the electrical conductivity of materials and techniques capable to measure electrical properties along different directions are required for samples with anisotropic electric transport properties. The most common method to measure the electrical conductivity of a sample is the two-probe technique that consists of contacting two probes or contacts on the specimen and measuring the voltage while a current is applied between the probes.[7] However, this measurement includes the voltage drop due to the electrical contact resistance between the probes and the sample that can be increasingly important as the electrical conductivity of the sample increases. To remove the influence of the contacts the four probe method has been used.[7] In this technique, while two probes are employed for passing current across the sample, the other two measure its voltage drop. A variety of four-probe methods have been developed for the electrical transport characterization of bulk and film samples either in their in-plane or cross directions (Figure 1).[2] For films with large areas and not extremely thin, or for bulk samples, the four probes are spaced equally (Figure 1(a)) and the separation distance must be much smaller than the sample size, otherwise correction factors must be included in the data reduction.[8–10] One of the main requirements for in-plane electrical conductivity measurements of films is the presence of an isolating substrate and, in some cases, a lithography process must be carried out to fabricate electrodes on the film, especially when the thickness of the film becomes smaller.[11,12] Some of the most typical techniques used to characterize in-plane films electrical properties are the Van der Pauw[13] and four probe method.[11,12] The Van der Pauw method[7] (VdP) (Figure 1(b)) uses four probes that are placed at the edges of an arbitrary shape film or bulk sample for in plane measurements of the sheet resistance. The current is passed across probes 1-2 while the probes 3-4 measure the voltage, or the current is passed across probes 1-4 and the voltage is measured across probes 3-2. The electrical conductivity is then determined from the sheet resistance knowing the sample thickness. A method to measure the out of plane conductivity of films is the modified transmission line model (TLM),[14,15] which originally was conceived to measure contact resistances.[16] This technique requires electrodes on top of structures etched in the film, which are separated by different distances (Figure 1(c)). The resistance measured between structures increases linearly with spacing while the vertical non-etched structures resistance remains unchanged. This makes possible the determination of the out of plane electrical conductivity of the film. Another out of plane method, that was originally used to measure contact resistances was presented by Cox and Strack.[17] This

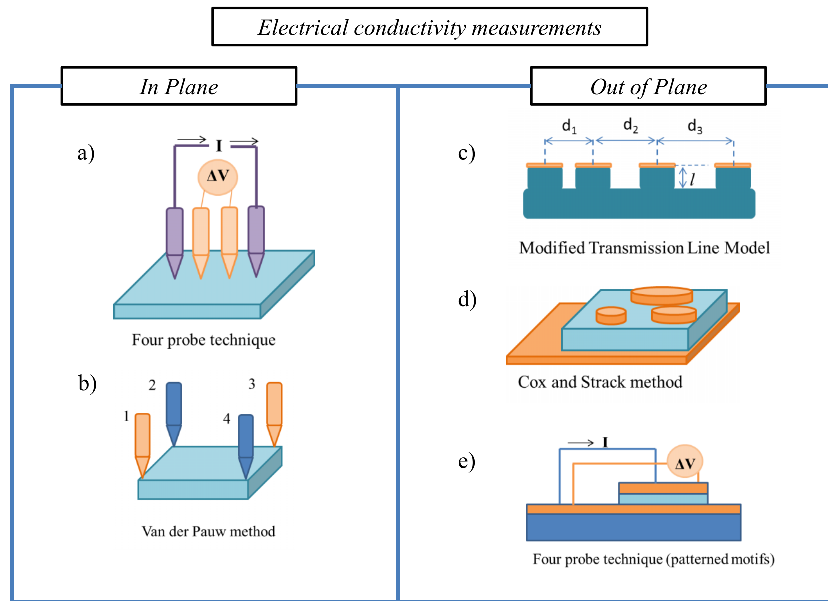

FIG. 1. Some of the techniques used to measure in plane and out of plane electrical conductivity of films and bulk samples. a) In-plane four point probe b) Van der Pauw c) Modified Transmission Line d) Cox and Strack and e) Cross-plane four probe technique.

method consisted of having an array of circular contacts on top of a sample, while its backside was contacted by a large surface area electrode (Figure 1(d)). This experimental set-up makes possible the separation of the spreading, contact and residual resistances from the total resistance measured. The cross-plane four probe method shown in Figure 1(e) employs a mesa structure for the film. For smaller sample sizes such as 1D structures or nanowires, conductive Atomic Force Microscopy (AFM) can be used to measure the voltage profile and back-out the contact resistance and electrical resistivity.[3] However, for the structure shown in Figure 1(e) possible non-uniform spreading of the current across the film and within electrodes, and the influence of the contact resistances between the interfaces[18,19] requires a careful analysis of the electric transport in the sample.

In this work, we used a four probe method to determine the out of plane electrical conductivity of thermoelectric Bi_2Te_3 films grown via electro-deposition process. Since in single bulk Bi_2Te_3 crystals the electric transport is highly anisotropic along the directions parallel ($1 \cdot 10^5$ S/m) and perpendicular ($0.3 \cdot 10^5$ S/m) to the c plane,[20] a setup to minimize current flow along different directions was designed for the film measurements. An anysotropy factor of around 4 is found between having the crystal oriented along the [0 0 1] or [1 1 0] directions. We fabricated film disc-shaped mesas with diameters ranging from 120 μm up to 80 μm and with different film thicknesses sandwiched between a common bottom electrode and a disc shaped top electrode for each mesa. While the disc geometry is similar to Cox and Strack, the use of mesa structures was selected to minimize current spreading into the in-plane direction of the film. A three-dimensional (3D) finite element model was used to predict the electric field distribution in the measured structures and take into account the non-uniform distribution of the current in the electrodes in the vicinity of the probes. The modeling shows that significant errors could arise in the measured film electrical conductivity if simpler one-dimensional models are employed, unless the electrode thickness and disc diameters are carefully selected. A high electrical conductivity of $(3.2 \pm 0.4) \cdot 10^5$ S/m is reported along the out of plane direction for the Bi_2Te_3 films.

II. EXPERIMENTAL WORK.

A. Fabrication Bi_2Te_3 films in shape of discs.

Electro-deposition conditions similar to the one published by C. V.Manzano *et al.*[21] were used to grow Bi_2Te_3 films with three different thicknesses, 4.6 ± 0.3 μm, 6.4 ± 0.7 μm and 7.2 ± 0.4 μm on 150 nm Pt layer held on Si substrates. Then, discs with 120 μm to 80 μm diameters were lithographically patterned in order to reduce the spreading of the electrical field across the film when passing a current across them. Photoresist (S1805) was spinned at 5000 rpm for 60 seconds, and pre-baked for one minute on a hot plate at 115°C. After exposure to ultra-violet light the MF-319 developer was used for 60 seconds to remove the exposed photoresist. Afterwards, 150 nm of gold was deposited by electron beam evaporation on top of the sample.

Finally, the photoresist was removed with acetone and we proceeded with the mesa etching with dilute nitric acid (1:3) for 5 minutes. Figure 2 shows Scanning Electron Microscopy (SEM) images of the discs obtained after this process.

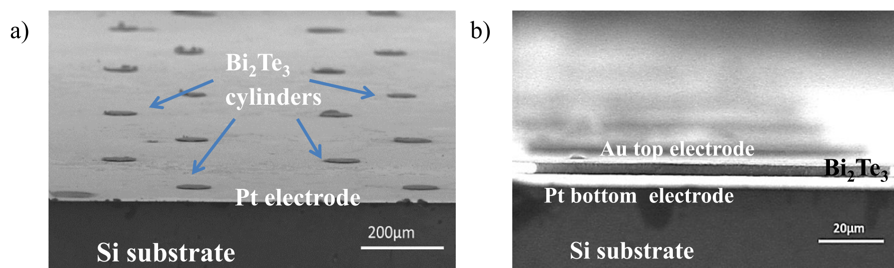

FIG. 2. a) Overview of patterned areas of the film and electrode structures obtained after the lithography process and mesa attack. b) Lateral view of one 100 μm diameter test structure.

B. Four Probe Station measurements.

The electrical conductivity measurements were carried out in a four probe station with a 4200-SCS Parameter Analyzer-Keithley. First, the electrical conductivity of the Pt and Au electrodes at the bottom and top sides of the film, respectively, were determined with the Van der Pauw (VdP) technique.[13] For that purpose, 150 nm of Pt and Au, equivalent to the electrodes size of the film-discs, were evaporated on squared (5 mm x 5 mm) Si wafers with oxide on its surface. Then, the probes of the station were positioned at the corners of the sample and the current-voltage curves measured as described in Ref. 13. We determined an electrical conductivity for the Pt film of $(3.1 \pm 0.2) \cdot 10^6$ S/m and for the Au film of $(3.6 \pm 0.1) \cdot 10^7$ S/m.

Then, we positioned carefully two probes on top of each disc while the other two were positioned on the bottom electrode. Figure 3(a) shows a schematic view of the experimental set up and Figure 3(b) shows an optical image of the position of the probes on a 120 μm diameter disc. Between the top and bottom current probes, a current ranging between $-1 \cdot 10^{-4}$ A and $+1 \cdot 10^{-4}$ A was passed across the sample while the voltage drop was recorded by the two voltage probes. For every disc, *I*-*V* curves were recorded and the electrical resistance determined from the slope of the curve.

During *I*-*V* measurements, optical images of the positions of the probes and the test structures were taken to determine the probes separation distances (Figure 3(b)). After the *I*-*V* measurements, imaging of the listed samples was carried out with SEM to check the status of the test structures after the probes were positioned on them. We observed that some structures were too scratched or broken to be used (Figure 3(c)). Another way to ensure non-damaging of the disc during measurements might consist of using a lateral camera with micrometer resolution that could help to perform a more sensitive approach of the probes to the surface of the disc. In any case, only the non-damage discs were taken into account for the analysis.

The electrical resistances (R_{exp}) obtained experimentally were plotted versus the thickness of the films. Figure 4 shows these resistances for three different film thickness and disc diameters

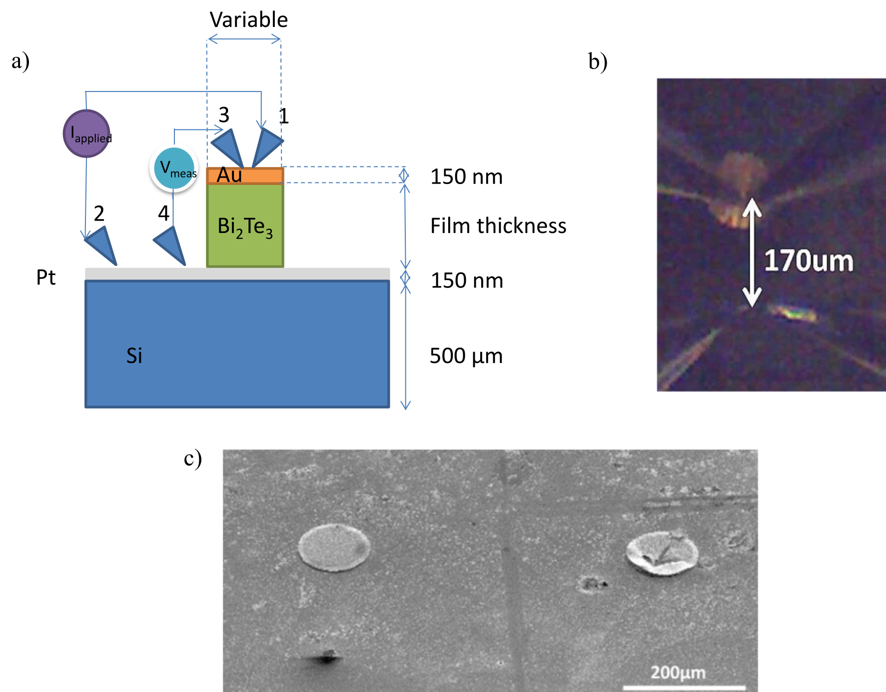

FIG. 3. a) Schematic view of the experimental set-up with the four probe station. b) Optical microscope image of the four probes positioning on a 120 μm disc-film whose thickness was 4.6 μm. The separation between top and bottom probes was 170 μm. c) SEM picture of two measured discs. The disc on the left side of the picture looks in good conditions after four probe measurements while the one on the right appears scratched and broken. Only the test structures that remained unaltered after each measurement were taken into consideration for the analysis.

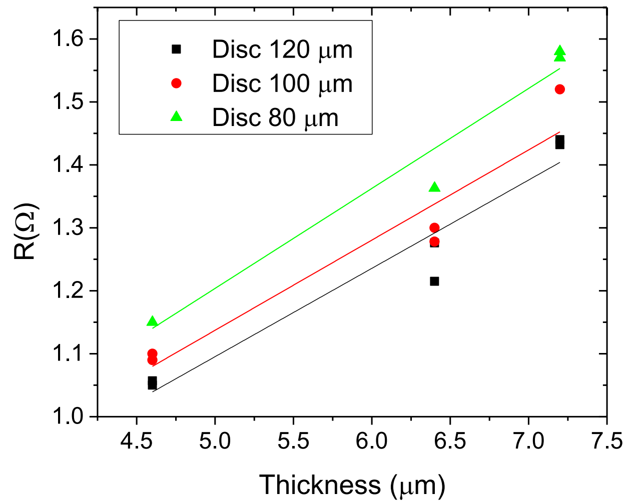

FIG. 4. Electrical resistances of different disc diameters versus the thickness of the films. The black squares, red circles and green triangles correspond respectively to 120 µm, 100 µm and 80 µm diameter discs. For 4.6 µm, 6.4 µm and 7.2 µm thicknesses, top to bottom probes distances were around 170 µm, 219 µm and 290 µm, respectively. Straight lines correspond to the linear fit of the data.

measured. A linear fit was drawn through the data. A deviation from linearity is observed, which indicates 3D spreading effects that are discussed in section II C.

C. Analysis and Discussion.

We developed a COMSOL® Multiphysics code to simulate the electrical transport measurements of the test structures and to determine the electrical conductivity of the Bi_2Te_3 films.

The geometry of the model consisted of an insulating substrate representing the oxide coated Si wafer ($\sigma = 1 \cdot 10^{-12}$ S/m) with a 150 nm layer of Pt on top with an electrical conductivity of $(3.1 \pm 0.2) \cdot 10^6$ S/m determined from the VdP measurements described in section II B. Then, the thermoelectric film with a thickness similar to each experimental sample was built on top of the Pt electrode, followed by an Au electrode of 150 nm thickness, whose electrical conductivity $(3.6 \pm 0.1) \cdot 10^7$ S/m was determined with the VdP technique in section II B.

Afterwards, two probes with 0.5 µm radius were positioned on top of the disc while the other probes were positioned at the bottom electrode separated by a known distance from the top probes. The separation between top and bottom probes was determined from optical images of the discs that were taken while performing four probe measurements (Figure 3(b)). Figure 5(a) shows the geometry of the COMSOL® model, while Figure 5(b) and 5(c) show the voltage distribution at the top and bottom electrodes.

We used the COMSOL® module "electrical currents" to define a current source at one of the top probes while defining a grounded probe at the bottom. The other two probes were used for measuring the voltage difference. Moreover, the effects of the electrical contact resistance were simulated using thin contact impedances at these boundaries, where one must define the resistivity and thickness of the contact. Finally, our theoretical model presents two unknown variables that must be fitted from experiments, i.e. the electrical conductivity of the film and the contact resistivity. For each sample, we varied each of these parameters within a range of possible values until the simulated electrical resistance, $R_{simulated}$, matched with the one obtained experimentally, R_{exp}, with less than 5% of difference. For simplicity, for each value of contact resistivity within the search range we fitted for the film electrical conductivity.

Figure 6 shows the fitted electrical conductivity of the film versus the electrical contact resistivity for the different film thicknesses and diameters of the discs.

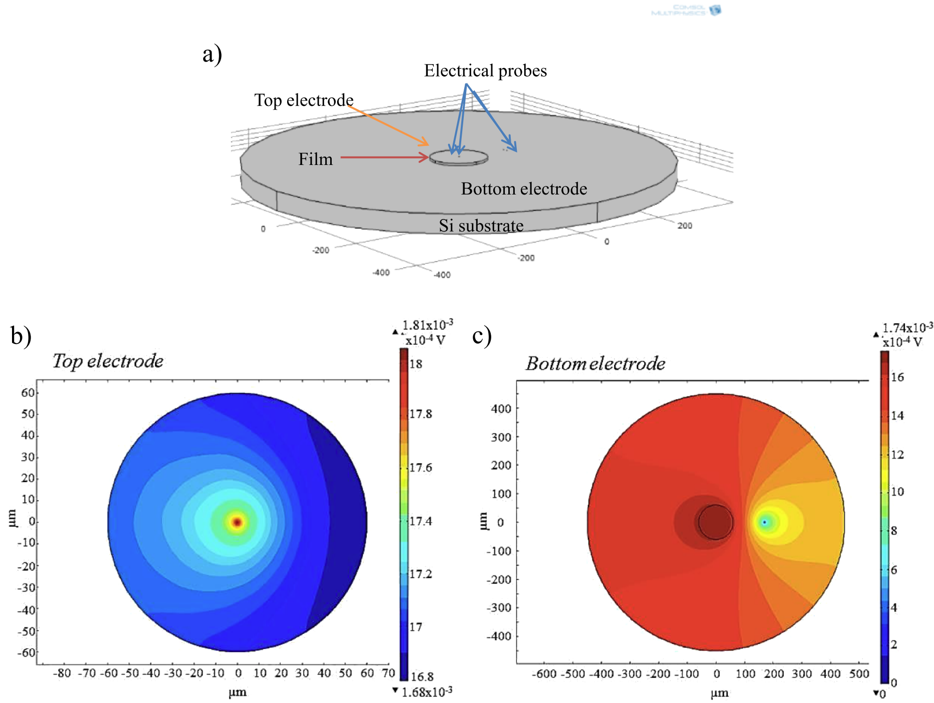

FIG. 5. a) Model geometry of the simulation. Voltage slices of the b) top and c) bottom electrodes, on top and underneath the sample respectively. The non-uniformity of the electrical voltage is indicated by the non-uniformity in color, particularly near the current probes locations.

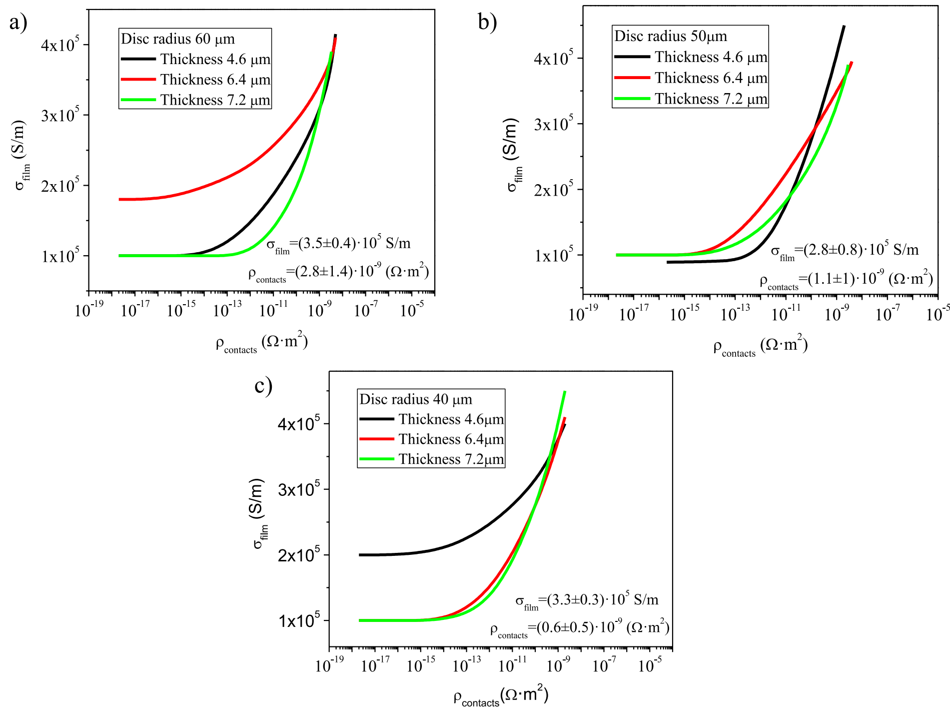

FIG. 6. Fitted electrical conductivity of the film (σ_{film}) versus the contact resistance per unit area (ρ_{contact}) for 4.6 µm, 6.4 µm and 7.2 µm film thickness determined for a set of a) 60 µm, b) 50 µm and c) 40 µm disc radius samples. For each disc radius the intersection of the curves provides a fitted value for electrical conductivity of the film and the contact resistivity.

While measurements performed for just one disc diameter may induce a relatively large uncertainty (see Figure 6), we considered individually the electrical conductivity of the film and contact resistivity per unit area of each diameter disc measured and carried out a statistical average. As a result, the averaged electrical conductivity obtained for the electro-deposited Bi_2Te_3 was determined to be: $<\sigma_{Bi2Te3_film}> = (3.2 \pm 0.4) \cdot 10^5$ S/m, while the averaged contact resistivity was $<\rho_{contact_resistance}> = (2 \pm 1) \cdot 10^{-9}\ \Omega \cdot m^2$. The uncertainty of the fitted results was obtained from the difference between the intersected points. Finally, the effect of the anisotropy of the film was also taken into account in the COMSOL® simulation. We carried out simulations with an in plane electrical conductivity of $\sim 7 \cdot 10^4$ S/m, which was determined experimentally, but the results show a variation of less than 1 % in comparison to the ones obtained without anisotropy.

The electrical conductivity of single crystal bulk Bi_2Te_3 as given in Ref. 20, for [1 1 0] is $\sim 0.3 \cdot 10^5$ S/m whilst for the [0 0 1] is $1 \cdot 10^5$ S/m, i.e. an anisotropy factor ~ 4 can be found. Our film presents an electrical conductivity in the out of plane direction [0 0 1] of $(3.2 \pm 0.4) \cdot 10^5$ S/m, which is ~ 3 times higher than reported for the bulk single crystal,[20] but the anisotropy factor with respect to the measurements performed in the in plane direction is ~ 4.5, which on the same order of magnitude of the one reported for a bulk single crystal.[20] This improvement can likely be explained by the high orientation of the electrodeposited Bi_2Te_3 films along the [1 1 0] direction in the in-plane of the film, as can be observed in Figure 7. Only the Pt/Si diffraction maxima from the electrode and the (1 1 0) and (2 2 0) diffraction maxima from Bi_2Te_3 can be identified. The (1 1 0) Bi_2Te_3 maxima is narrow indicating a high crystallinity. The fact that we can observed the second order is indicative of a highly texture film. Moreover, the electrochemical deposition technique uses an electric field during the growth. The electric field can favor the growth of Bi_2Te_3 grains oriented along the highest electrical conductivity direction. Regarding the contact resistance, its result was observed to be similar to the best resistance per unit area measurements found in literature, which are estimated to be between 10^{-8} to $10^{-9}\ \Omega \cdot m^2$.[22,23]

Next we investigated under what conditions a simpler one-dimension electrical transport model could be used to fit the experimental results accurately. The one-dimensional (1D) transport yields, $R = \rho \cdot \frac{l}{A}$ where R is the electrical resistance, ρ the electrical resistivity and l and A the length and area of the sample, respectively. This model indicates that the measured resistance should be linear with the thickness of the film, which is not the case in Figure 4. To find the reason for this trend we used our COMSOL® results and determined the voltage drops across the top electrode, the film, and the bottom electrode. Then the COMSOL® voltages were used to calculate the electrical resistance contributions due to each layer and we compared these results with predictions of the 1D model. The electrical resistance of the film expressed with the 1D-theory yields,

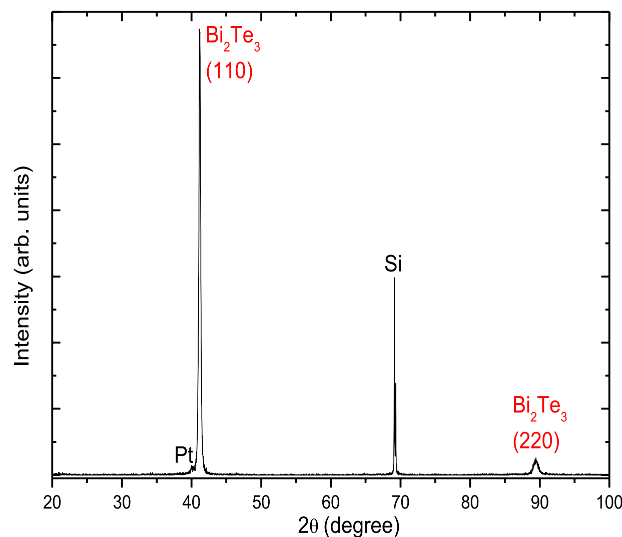

FIG. 7. Example of X-Ray diffraction of highly oriented Bi_2Te_3 electrodeposited films used in this study.

$$R_{total} = \rho_{top\ elc} \cdot \frac{l_{elec}}{A_{elec}} + \rho_{film} \cdot \frac{l_{film}}{A_{film}} + \rho_{bot\ elc} \cdot \frac{l_{elec}}{A_{elec}} \tag{1}$$

where R_{total} is the total resistance across film and electrodes, $\rho_{top\ elc}$, $\rho_{bot\ elc}$ and ρ_{film} the electrical resistivity of top and bottom electrodes and film, respectively, and l_{elc} , l_{film} and A_{elc} , A_{film} are the length and the area (perpendicular to the current direction) of the electrodes and the film, respectively.

As seen in Figure 5(b) at the top electrode, the current probe with 0.5 µm radius causes a necking effect that prevents a fully uniform voltage distribution of the surface. The thicker the electrode is, the more uniform is the voltage on the surface. Figure 8(a) shows the voltage drop across the film and electrodes in its cross plane direction, while Figure 8(b) displays the voltage obtained along the radius of the film at its top and bottom faces for a 4.6 µm thickness film. From these figures, a discrepancy between COMSOL® and the 1D theory of around 1% was found for the Au (first term in Eq.(1)) and Pt (third term in Eq.(1)) electrodes with 150 nm thickness, while a discrepancy of around 11% was found for the thermoelectric film contribution (second term in Eq. (1)). Even though there seem to be so far a good agreement between theory and simulation, these elements contribute less than 5% to the total resistance determined between probes. The larger contribution to the total resistance comes from the Pt electrode resistance along its in-plane surface, between the center of the disc and the bottom probes. Figure 8(c) shows the voltage drop at the bottom electrode from the center of the film to the grounded probe positioned at 170 µm. This contribution is not contemplated in the 1D-analysis (Eq. (1)). In order to consider the effect of the field spreading and the resistance influence at the bottom electrode, one must solve the analytical expression coming from Laplace's equation for constriction resistance obtained for non-quantum

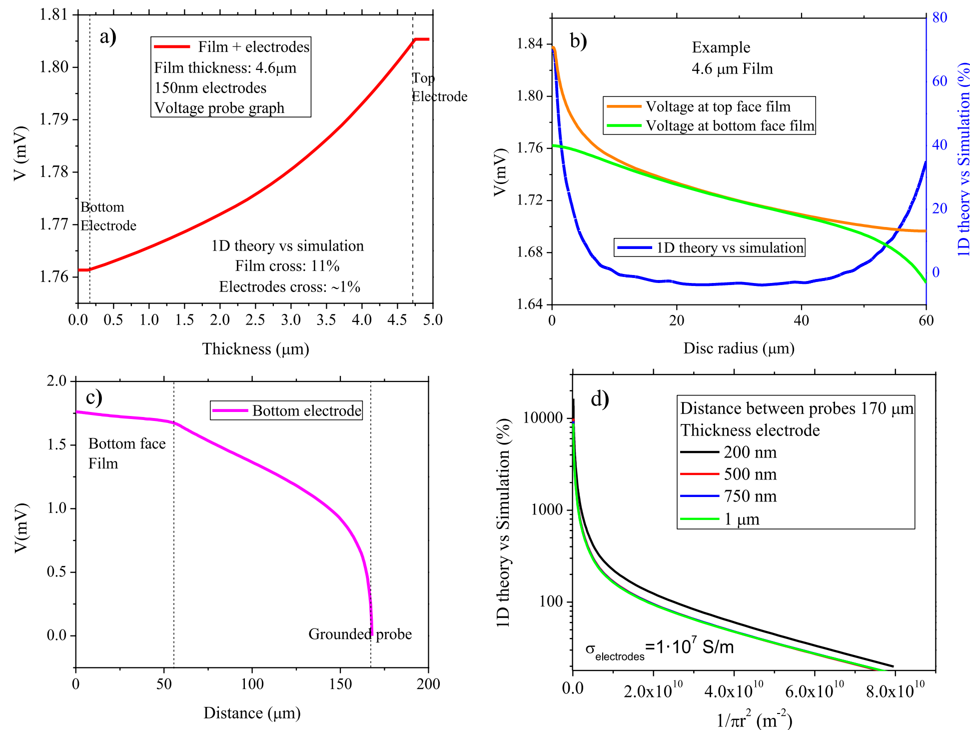

FIG. 8. a) Voltage drop just across the electrodes and the film from the top voltage probe, separated 3µm from the top current probe, to the bottom of the sample. A discrepancy of 11 % and 1 % respect to the 1D theory is observed for the film and electrodes, respectively. b) Voltage along the film radius at its top and bottom faces. The discrepancy between the 1D theory and the simulation varies along this distance. c) Voltage drop along the bottom electrode from the center of the film disc to the grounded probe. d) Discrepancy between the simulation and 1D-theory results for the electrical resistance of a 4.6 µm thickness sample with an electrical conductivity of $1 \cdot 10^5$ S/m and both electrodes with the same variable thickness but same electrical conductivity, $1 \cdot 10^7$ S/m. The distance between top to bottom probes is 175 µm.

contacts.[24] This analytical study is complicated whilst our 3D simulation takes this effect already into account simplifying the analysis. If the electrode was fully energized and the bottom probes were very close to the disc, the result obtained from the 1D theory would match better with the electrical conductivity of the film. Larger probes with diameters similar to those of the discs studied could be used for that purpose.

In order to find out if the discrepancy between the 1D model and COMSOL® can be alleviated by using electrodes with larger thicknesses, Figure 8(d) shows the difference between the simulation and the 1D theory calculated for a 5 µm film with an electrical conductivity of $1 \cdot 10^5$ S/m and electrodes with identical thicknesses and electrical conductivity of $1 \cdot 10^7$ S/m and distance (kept constant for all simulations in Figure 8(d)) between top and bottom probes of 170 µm. The percentage of discrepancy between theory and simulation has been calculated according to the expression,

$$1D\ Theory\ vs\ Comsol\ Simulation\ (\%) = \left(\frac{R_{theory} - R_{simulation}}{R_{theory}} \right) \cdot 100 \tag{2}$$

where $R_{theory} = \rho_{film} \cdot \frac{l_{film}}{A_{film}}$ is the resistance of the film calculated from the 1D theory while $R_{simulation}$ is the resistance obtained from the simulation.

In Figure 8 we observe that the discrepancy decreases monotonically in all cases when the diameter of the film reduces as well as when the thickness of the electrode increases, as it approaches to the 1D case. As an example, a 2 µm radius film involves a discrepancy between the simulation and the 1D theory of around 14 % and 25 % for the 1µm and 200 nm thickness electrodes, respectively. Therefore, radiuses below that and electrodes as thick as possible are required for a proper estimation of the electrical conductivity of the film with the 1D theory.

Therefore, the effect of the field spreading in the electrodes becomes extremely important, especially at the bottom electrode one, and has an important influence in the total resistance as the radius of the film becomes bigger than 2 µm.

III. CONCLUSIONS.

Out of plane electrical conductivity measurements for highly anisotropic films, such as the high electrical conductivity Bi_2Te_3 films measured here, requires well designed experimental set-ups. We have investigated the use of a four probe method to carry out electrical measurements of electrodeposited Bi_2Te_3 films with different thicknesses. We proposed the fabrication of film-discs via lithography and mesa patterning with different diameters to avoid the current flow along the plane, but with diameters big enough to allow positioning the probes on top of them. The electrical resistances measured from the I-V curves of the film-discs were fitted with a COMSOL® finite element model that determined an electrical conductivity for the film of $(3.2 \pm 0.4) \cdot 10^5$ S/m, around four times higher than its in plane direction. This value was compared with other results given in literature for bulk material with the same crystalline orientation [1 1 0]. We observe that our result is around three times higher than the single crystal bulk Bi_2Te_3 one found in literature ($\sim 1 \cdot 10^5$ S/m), and we attribute the high conductivity to the possibly superior alignment and crystallinity of the films. As it has been observed, the anisotropy involves large differences in the transport properties depending on the direction in which they are studied. Therefore, a proper characterization of the electrical and thermal properties in the different directions of such materials must be carried out to fully determine its performance. The contact resistance was simultaneously determined with this technique, $\langle \rho_{contact_resistance} \rangle = (2 \pm 1) \cdot 10^{-9}\ \Omega \cdot m^2$, which is in good agreement with those values found in literature (10^{-8} - $10^{-9}\ \Omega \cdot m^2$).

Moreover, the simulation reveals that the 1D-theory underestimates the value of the electrical conductivity of the film and the discrepancy increases as the disc radius increases and electrode thickness decreases. The main source for this discrepancy comes from the influence of the bottom electrode in its in-plane direction whose contribution to the total resistance is much larger than the film and has to be taken into account using the 3D simulation.

ACKNOWLEDGEMENTS

M.M.G. wants to acknowledge support from ERC StG NanoTEC 240497. M.M.R. acknowledges CSIC for his JAE Pre-Doctoral fellowship. T.B.T. gratefully acknowledges funding from the U.S. Department of Energy, Office of Science, Office of Basic Energy Sciences through the S3TEC Energy Frontiers Research Center at MIT under Award No. DE-SC0001299.

[1] D. M. Rowe, *CRC Handbook of Thermoelectrics* (CRC Press, Boca RatonFL , USA, 1995).
[2] Je-Hyeong Bahk, Tela Favaloro, and Ali Shakouri, Annual Review of Heat Transfer **16**(1), (2013).
[3] Miguel Muñoz Rojo, Olga Caballero Calero, A. F. Lopeandia, J. Rodriguez-Viejo, and Marisol Martin-Gonzalez, Nanoscale **5**, 11526 (2013).
[4] Yuanjian Zhang, Toshiyuki Mori, Jinhua Ye, and Markus Antonietti, Journal of the American Chemical Society **132**(18), 6294 (2010).
[5] Lu Huang, Yi Huang, Jiajie Liang, Xiangjian Wan, and Yongsheng Chen, Nano Res. **4**(7), 675 (2011).
[6] H. Julian Goldsmid, *Introduction to Thermoelectricity* (Springer Berlin Heidelberg, 2010), Vol. 121, p. 139.
[7] Yadunath Singh, International Journal of Modern Physics: Conference Series **22**, 745 (2013).
[8] Dieter K. Schroder, *Semiconductor material and device characterization* (John Wiley & Sons, New Jersey, 2006).
[9] Standard method for measuring resistivity of silicon slices with a collinear four-point probe. (Annual Book of ASTM Standards, West Conshohocken, PA, 1996).
[10] M. P. Albert and J.F. Combs, IEEE Transactions on Electron Devices **ED-11**(148), (1964).
[11] Paul V. Pesavento, Reid J. Chesterfield, Christopher R. Newman, and C. Daniel Frisbie, Journal of Applied Physics **96**(12), 7312 (2004).
[12] Anastassios Mavrokefalos, Michael T. Pettes, Feng Zhou, and Li Shi, Review of Scientific Instruments **78**(3), (2007).
[13] A. A. Ramadan, R. D. Gould, and A. Ashour, Thin Solid Films **239**(2), 272 (1994).
[14] B. Yang, W. L. Liu, J. L. Liu, K. L. Wang, and G. Chen, Applied Physics Letters **81**(19), 3588 (2002).
[15] Rama Venkatasubramanian, Edward Siivola, Thomas Colpitts, and Brooks O'Quinn, Nature **413**(6856), 597 (2001).
[16] H. H. Berger, Solid-State Electronics **15**(2), 145 (1972).
[17] R. H. Cox and H. Strack, Solid-State Electronics **10**(12), 1213 (1967).
[18] Luciana W. da Silva and Massoud Kaviany, International Journal of Heat and Mass Transfer **47**(10-11), 2417 (2004).
[19] Ya-Huei Chang, Shien-Ping Feng, Jian Yang, Bed Poudel, Bo Yu, b Zhifeng Ren, and Gang Chen, Physical Chemistry Chemical Physics **15**, 6757 (2013).
[20] A. Jacquot, N. Farag, M. Jaegle, M. Bobeth, J. Schmidt, D. Ebling, and H. Böttner, Journal of Elec Materi **39**(9), 1861 (2010).
[21] C.V. Manzano, A. Rojas, M. Decepida, B. Abad, Y. Feliz, O. Caballero-Calero, D.A. Borca-Tasciuc, and M. Martín-González, J Solid State Electrochem **17**(7), 2071 (2013).
[22] R. Melamud, A.M. Pettes, and S. Higuchi, 26th International Conference on Thermoelectrics (ICT) (2007).
[23] Miguel Muñoz-Rojo, Olga Caballero-Calero, and Marisol Martín-González, Applied Physics Letters **103**(18), (2013).
[24] Frank G. Shi A. Mikrajuddin, H.K. Kim, and Kikuo Okuyama, Materials Science in Semiconductor Processing **2**(4), 321 (1999).